 doi:10.20944/preprints202207.0094.v1

Design simulation and data analysis of an optical spectrometer

Muddasir Naeem[1*], Tayyab Imran[1], Mukhtar Hussain[2], Arshad Saleem Bhatti[3]

[1]*Group of Laser Development (GoLD), Department of Physics, Syed Babar Ali School of Science and Engineering, Lahore University of Management Sciences (LUMS), Lahore 54792, Pakistan. muddasirnaeem98@gmail.com (M.N.); tayyab_imran@lums.edu.pk (T.I.)*

[2]*Department of Physics, University of Central Florida, Orlando, FL 32816, USA. mukhtar.hussain@ucf.edu (M.H.)*

[3]*M.A. Jinnah Campus, Virtual University, Defence Road, Off Raiwind Road, Lahore 54660, Pakistan. asbhatti@comsats.edu.pk (A.S.B.)*

**Corresponding Author: Muddasir Naeem*

"The authors to whom correspondence may be addressed: muddasirnaeem98@gmail.com"

Abstract – Spectrometers have a wide range of applications ranging from optical to non-optical spectroscopy. The need for compact, portable, and user-friendly spectrometers has been the pivot of attention from small laboratories to the industrial scale. Here, the Czerny Turner configuration-based optical spectrometer simulation design is carried out using ZEMAX OpticStudio. A compact and low-cost optical spectrometer in the visible range has been developed by using diffraction grating as a dispersive element and USB-type WebCAM CCD (Charge-coupled device) as a detector instead of an expensive commercial diffraction grating and detector. Using National Instruments LabVIEW, data acquisition, processing, and displaying techniques are made possible. We have employed different virtual images in LabVIEW programs to collect the pixel-to-pixel information and wavelength-intensity information from the image captured using the WebCAM CCD. Finally, we have shown that the OpticStudio-based spectrometer and experimental measurements of the developed spectrometer are in good agreement.

Keywords – ***Spectrometer, NI LabVIEW, Virtual Image (VI), Diffraction Grating, ZEMAX***.

1. INTRODUCTION

Spectrometers are used to measure the light of different wavelengths over a wide range of the electromagnetic spectrum. It is widely used to analyze material by spectroscopy. C. R. Masson developed a low-cost acoustic optical spectrometer for millimeter-wave observation with an effective resolution of 160 kHz [1]. Arzhantsev, S., and Maroncelli developed and characterized a spectrometer based on an optical Kerr shutter for emission gating, and a polychromatic plus charge-coupled device (CCD) detection system for recoding the time-resolved emission spectra of fluorescence species [2]. An acoustic-optical spectrometer was designed and tested for solar radio astronomy and variability studies of cosmic masers sources with a 5-meter antenna (RT5) [3]. An imaging spectrometer based on the curved prism configuration has been modeled, showing the imaging quality factors influencing [4]. The imaging spectrometer is an optical instrument that can simultaneously measure spectral and spatial properties. Because of its dimensional reliability and low cost, the prism-based dispersive spectrometer is one of the most used techniques in remote sensing. A micro-optical spectrometer in the spectral range of (200-910) nm is developed, which has a resolution of ~ 1 nm [5]. To improve the spectral resolution, an Offner spectrometer based on the geometrical study of ring fields was developed and the analytical architecture

 doi:10.20944/preprints202207.0094.v1

was demonstrated using the optical design program Code V to construct a spectrometer ranging from 900 to 1700 nm [6]. The concept and design of an integrated optical device featuring evanescent field sensing and spectrometric analysis were presented by Gloria Mico [7]. Such an integrated optics sensing spectrometer (IOSS) consists of a modified arrayed waveguide grating (AWG) whose arms are engineered into two sets having different focal points. Two reference designs are provided for the visible and near-infrared wavelengths, aimed at the determination of the concentration of known solutes through absorption spectroscopy. Recently, we designed the Czerny–Turner Configuration-Based Raman Spectrometer by using Zemax based on the physical optics propagation algorithm [8], yet the experimental validation of such spectrometer was required to implement.

Here, we present the design, simulation and development of a compact and low-cost optical spectrometer with data acquisition and analysis using NI LabVIEW. The simulations are carried out using Zemax OpticStudio. The spectrometer results are recorded in the form of images and then analyzed using different tools in NI LabVIEW and compared with the Zemax OpticStudio results.

2. GENERAL VIEW OF AN OPTICAL SPECTROMETER

Czerny Turner configuration is one of the compact and flexible spectrometer designs which consists of a single detector instead of a detector array and requires fixed components, as shown in Fig. 1(a). Czerny Turner Spectrometer consists of one plane diffraction grating and two concave mirrors. The first mirror is a collimating mirror that collimates the beam and makes it equivalent to the grating surface of the spectrometer. The following mirror is the focusing mirror that focuses the input light from the source to the image sensor.
Initially, the wavelength range is selected, and then the center wavelength is calculated as follows;

$$\lambda_2 - \lambda_1 = \Delta\lambda \quad ; \quad \lambda_c = \frac{(\lambda_2 - \lambda_1)}{2} \tag{1}$$

If the deviation angle $(\theta) = 0$, then it will be the Littrow configuration [9]. According to the deviation, angles α and β are calculated.

$$\alpha = \sin^{-1}\left[\frac{\lambda_c G}{2} cos\left(\frac{\theta}{2}\right)\right] - \frac{\theta}{2} \tag{2}$$

$$\beta = \theta - \alpha$$

Then one must choose the detector size according to the size of the spectrometer. After choosing detector size, the focal length of focusing mirror L_F is obtained as,

$$L_F = L_D \frac{\cos(\beta)}{G(\lambda_2 - \lambda_1)} \tag{3}$$

The focal length of collimating mirror Lc is calculated as,

$$L_c = L_F\left[\frac{\cos(\alpha)}{\cos(\beta)}\right] \tag{4}$$

By using the collimating mirror L_C, the slit width is obtained as,

$$W_{slit} = G(\Delta\lambda)\frac{L_c}{\cos(\alpha)} \tag{5}$$

 doi:10.20944/preprints202207.0094.v1

Here G is the grating constant, W_{slit} is the slit width, which is the entrance slit for any optical light. The careful selection of the slit width is an important factor when designing and developing a spectrometer [10].

3. DESIGN AND SIMULATIONS OF OPTICAL SPECTROMETER

The design and simulations of the spectrometer are carried out using the ZEMAX OpticStudio [11] software. The parameters of each optical component defined in the lens data editor window are calculated as per the mathematical model described in the previous section, as shown in Table 1.

Table 1. Lens data editor window for the design of an optical spectrometer in OpticStudio

Surf: Type		Comment	Radius [cm]	Thickness [cm]	Semi-Diameter [cm]	Lines/µm
OBJ	Standard	Source	Infinity	0.90	0.00	
1	Standard	Entrance slit	Infinity	4.55	0.08	
2	Standard	Collimating mirror	-10	-3.00	0.61	
3	Diffraction Grating	Diffraction grating	Infinity	3.00	0.52	0.600
4	Standard	Focusing mirror	-10	-4.55	0.61	
IMG	Standard	Detector	Infinity	-	0.30	

We have set the surface type to standard except for the diffraction grating surface. Values of parameters present in the Lens Data Editor (LDE) are according to the designed spectrometer. After defining the required surface and other relevant parameters involved in the design, the software provides a pictorial layout of the spectrometer as shown in Fig. 1(b). This includes the source, input slit, collimating mirror, diffraction grating, focusing mirror and image at the last surface (Detector).

The design and simulation of the spectrometer are carried out using Physical Optics Propagation (POP) algorithm for three different wavelengths 0.5 µm, 0.6 µm and 0.7 µm. The spectrometer simulation is carried out using diffraction grating of 600 lines/mm. For the designed spectrometer image-space NA, object space NA, image-space F/#, total tracks and stop radius are 0.094, 0.088, 39.0625, 4.5 and 0.08 mm respectively.

Preprints (www.preprints.org) | NOT PEER-REVIEWED | Posted: 6 July 2022 doi:10.20944/preprints202207.0094.v1

4. SIMULATION RESULTS OF THE SPECTROMETER (VISIBLE RANGE)

4.1. Spot Diagram

The variation in the size of the spot by changing the position of the detector is shown in Fig. 1(c). A focused spot will be obtained if the detector is placed at the mirror's focal point.

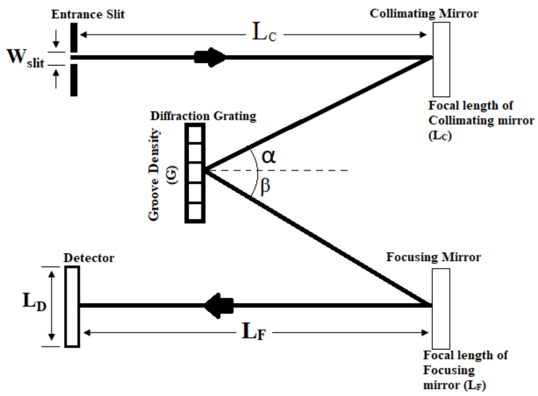

(a)

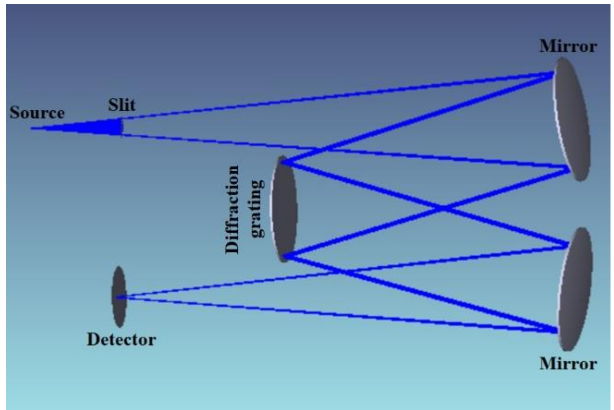

(b)

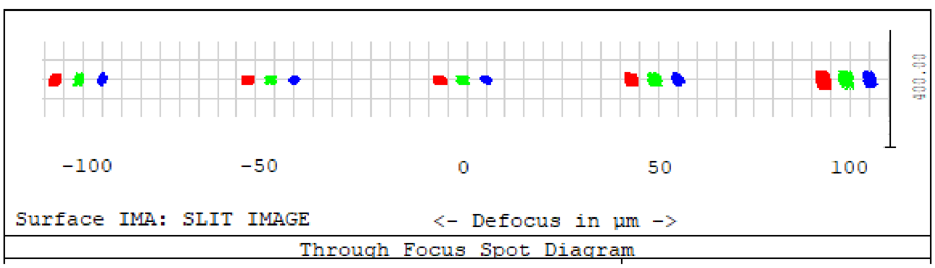

(c)

Fig. 1: (a) Schematic representation of Czerny-Turner configuration-based spectrometer **(b)** schematic of the simulated design of the spectrometer in OpticStudio **(c)** Variation in spot diagram relative to the distance of the detector from the focus point of focusing mirror.

When we move the detector towards or away from the focusing mirror, the spot size on the detector varied as shown in Fig. 1(c). The target's geometrical representation becomes a finite blur spot in a decreased resolution when the detector is not in the paraxial region. As the separation between these planes increases, the blur spot gets more prominent, and resolution decreases further.

4.2. Image of the Spectral Irradiance

Spectral irradiance is the irradiance of the surface per unit frequency or wavelength.

Preprints (www.preprints.org) | NOT PEER-REVIEWED | Posted: 6 July 2022 doi:10.20944/preprints202207.0094.v1

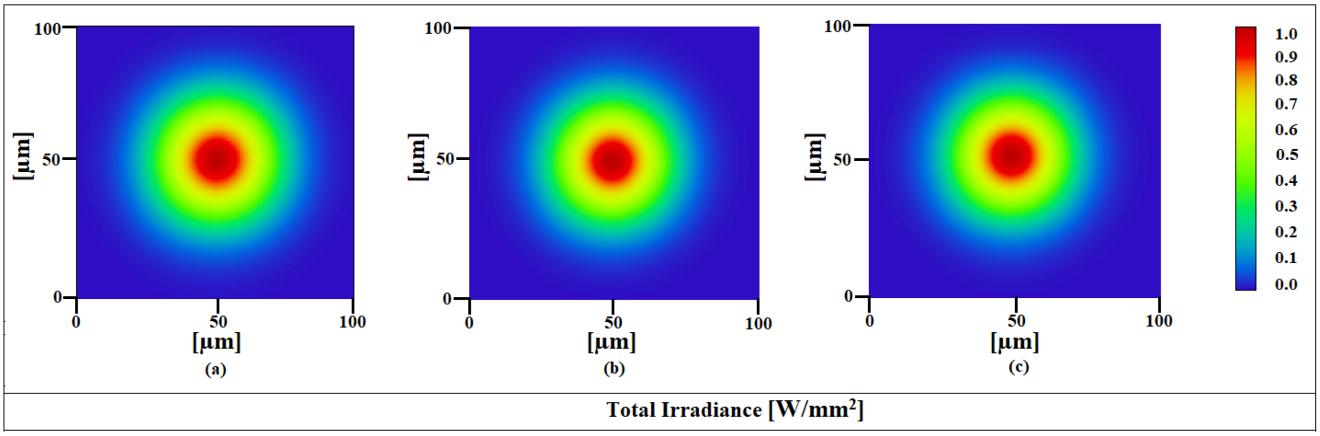

Fig. 2: Image of the spectral irradiance on the detector at **(a)** $\lambda = 0.5\ \mu m$ **(b)** $\lambda = 0.6\ \mu m$ **(c)** $\lambda = 0.7\ \mu m$

The spot size at 0.5 μm, 0.6 μm and 0.7 μm respectively in terms of total irradiance at the surface of the detector is shown in Fig. 2. Irradiance at the center is maximum because most of the rays are focused at the center; moving away from the center will decrease the irradiance and energy per unit area delivered to the surface also decreases [12, 13]. The images of the spectral irradiance showed that the aberration is minimum in the optical range.

5. EXPERIMENTAL SETUP AND RESULTS

The schematic layout of the spectrometer setup is shown in Fig. 3(a) consists of two concave mirrors, diffraction grating, white light LED as a source, and a Webcam without a lens as a CCD detector. The radius of curvature of the mirrors is 10 cm and diffraction grating of grating constant of 600 lines/mm is used. USB Webcam CCD is used as a detector to acquire the image through NI LabVIEW. NI LabVIEW is used to record the results in the form of an image and further analyze the results using different tools in LabVIEW [14, 15]. NI LabVIEW gives us an easy and user-friendly interface through which we can process data by using different VI's (Virtual Image).

5.1. Acquisition of Image

The image of the output spectrum in acquired using NI-IMAQ tools in LabVIEW. Three methods for acquiring images in the NI-IMAQ tool can be adopted: snap, grab, and sequence modes. The snap method takes a single image for each retrieval while the grab method captures the number of images, but only one image is taken for processing. Using the sequence method, only particular images can be acquired, and further processed [16]. The easiest mode for image acquisition is a snap acquisition, which has been considered in our acquisition which takes only one image for processing [17].

Preprints (www.preprints.org) | NOT PEER-REVIEWED | Posted: 6 July 2022 doi:10.20944/preprints202207.0094.v1

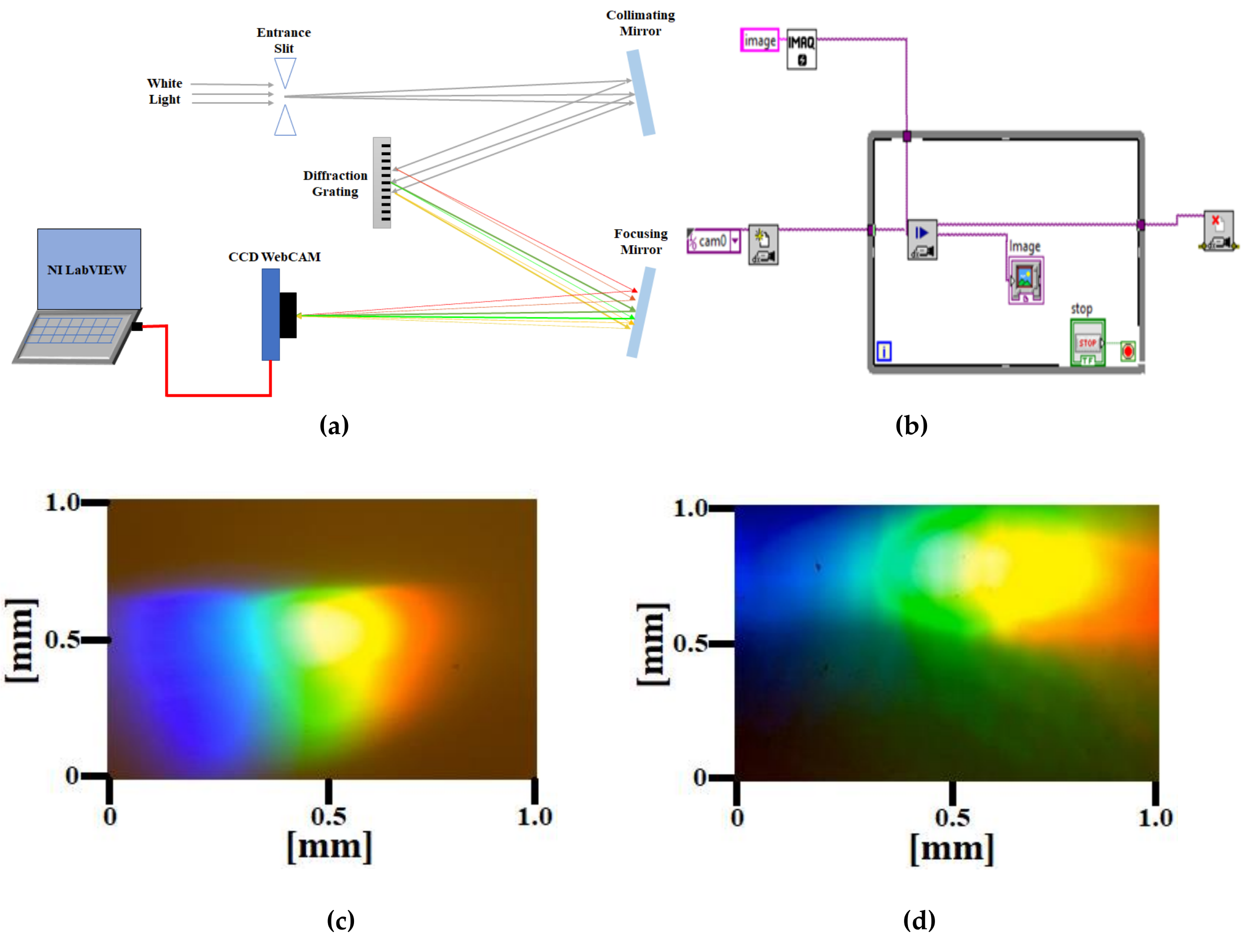

Fig. 3: (a) Schematic of the experimental setup of the Czerny-Turner configuration based optical spectrometer **(b)** Block diagram in LabVIEW for the image acquisition in snaps **(c)** Image of spectrum acquired using NI LabVIEW program for a prism as dispersive element **(d)** Image of spectrum acquired using NI LabVIEW program for diffraction grating as a dispersive element.

The block diagram in LabVIEW for the image acquisition in snap mode is shown in Fig. 3(b), which consists of IMAQ Snap, IMAQ Create, Image screen and IMAQ CloseCamera which is used to acquire a snap through the camera. Using a while loop with these VI's, we have continuously acquired the acquisition. The snap method for image acquisition begins with the initialization stage, first, a session-in VI is used which specifies the camera to open. We are using a USB Webcam so cam0 is identified as a default. IMAQ Create VI creates a temporary memory location for an image. IMAQ Snap VI takes the snap when the camera is open [16]. The image will appear on the image screen VI. In the end, IMAQ CloseCamera VI is placed which closes the camera after taking the required snap. With the IMAQ Snap VI in the while loop, the continuous snap will be recorded until the while loop is stopped using the STOP button [17].

We have alternatively tested our imaging spectrometer by using prism and diffraction grating. Images recorded from the optical spectrometer using prism and diffraction grating are shown in Figs. 3(c) and 3(d) respectively. The images obtained from the grating-based spectrometer is dispersive than from the prism-based spectrometer.

Preprints (www.preprints.org) | NOT PEER-REVIEWED | Posted: 6 July 2022 doi:10.20944/preprints202207.0094.v1

6. ANALYSIS OF EXPERIMENTAL RESULTS BY USING LABVIEW

6.1. Formation of Array having Pixel to Pixel and corresponding Graph

In the initial phase, we acquired the image using the program in NI LabVIEW. Then different VI's have been used to process the acquired image and obtain pixel-to-pixel values. For this, a program is designed using different VI's to make a graph that displays the intensity of each pixel. The designed program can pick pixels values from the given image and form an array of pixels [18, 19]. To get the pixels in the graphical form we have designed a program using VI's in NI LabVIEW which gives a graph (spectrum) of the pixels. We have used VI of IMAQ Create, IMAQ ReadFile, Invoke Node, IMAQ LineProfile and IMAQ Dispose. We have used a while loop, case structure, an array, mathematical and logical operations in this VI.

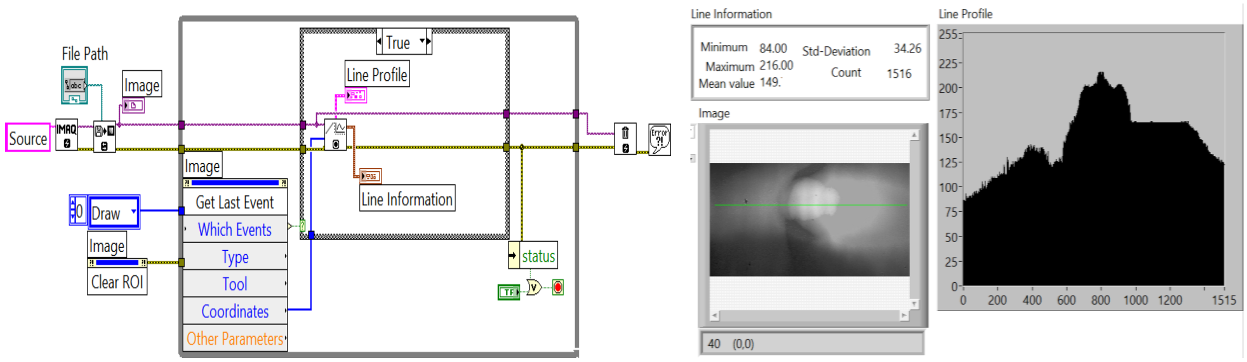

(a) **(b)**

Fig. 4: (a) Block diagram for the line information of pixels **(b)** Green line is drawn on the image to observe the line graph

The block diagram of the program for the acquisition of the graph from pixels is shown in Fig. 4(a). First IMAQ ReadFile VI takes the image from the address given in the file path. IMAQ Create VI makes a temporary memory file of the image to process it further. Then Invoke Node VI defines the event (draw line) and gives coordinates of the line (region of interest) drawn on the image screen. In the case structure, IMAQ LineProfile is used which calculates the profile of a line of pixels. This VI returns a data type (cluster) compatible with the LabVIEW graph. The relevant pixel information is taken from the specified line. The IMAQ LineProfile VI is used which gives the value of the pixels at the given coordinates in graphical form. The IMAQ LineProfile VI only processes the grayscale images so first, it converts the input image into the grayscale image and then gives the values of pixels at the coordinate selected in the image. IMAQ Dispose and Error Handler VI are placed outside the While loop to remove the extra coordinates that are not running in the loop. Nor gate condition is applied to case structure; if it is true then case structure will give output; otherwise, it will stop.

The green line drawn on the image screen shows that pixels are collected from the part of the image covered by the green line. The line graph of pixels is shown in Fig. 4(b) which shows the variation of pixels on the image. The small window on the upper left of Fig. 4(b), gives the information about the maximum pixels, minimum pixels, and deviation in the pixels value in the graph.

Preprints (www.preprints.org) | NOT PEER-REVIEWED | Posted: 6 July 2022 doi:10.20944/preprints202207.0094.v1

6.2. *Color Spectrum of RGB (color) Image*

We have designed a program using different VI's in NI LabVIEW which gives a wavelength intensity graph of the image. The block diagram to record the spectrum from the RGB image is shown in Fig. 5(a). The designed program used different VI's such as IMAQ Create, IMAQ ReadFile, Invoke Node, IMAQ ColorLearn and IMAQ Dispose. We also used a for loop, while loop, case structure, arrays, mathematical and logical operations. First IMAQ ReadFile VI Reads an image file from the address given in the file path. The file format can be a standard format such as BMP, TIFF, JPEG, JPEG2000, PNG, etc., or a nonstandard format known to the user. File-path is the complete pathname, including drive, directory, and filename, of the file to read. After that IMAQ Create VI specifies the image type, name and makes a temporary memory file of the image to process it further. Then Invoke Node VI is used to define the event invoke a method or action on an ROI. In the first case structure, IMAQ ColorLearn VI is used which extracts the color features of an image, This can be used for color matching or other applications related to color information, such as color identification and color image segmentation.

In ColorLearn VI, the image is a reference to the color image to learn color information; color sensitivity specifies the sensitivity of the color information in the image. When the loop runs at low sensitivity, it can collect 16 colors from the selected image. There can be 32 colors in the medium sensitivity loop, and in the high sensitivity loop, it will pick 58 colors. Learn saturation threshold specifies the threshold value to distinguish two colors with the same intensity value. Color spectrum returns the color features found in the image region. These features represent the color information in the image region in a compact form [18, 19].

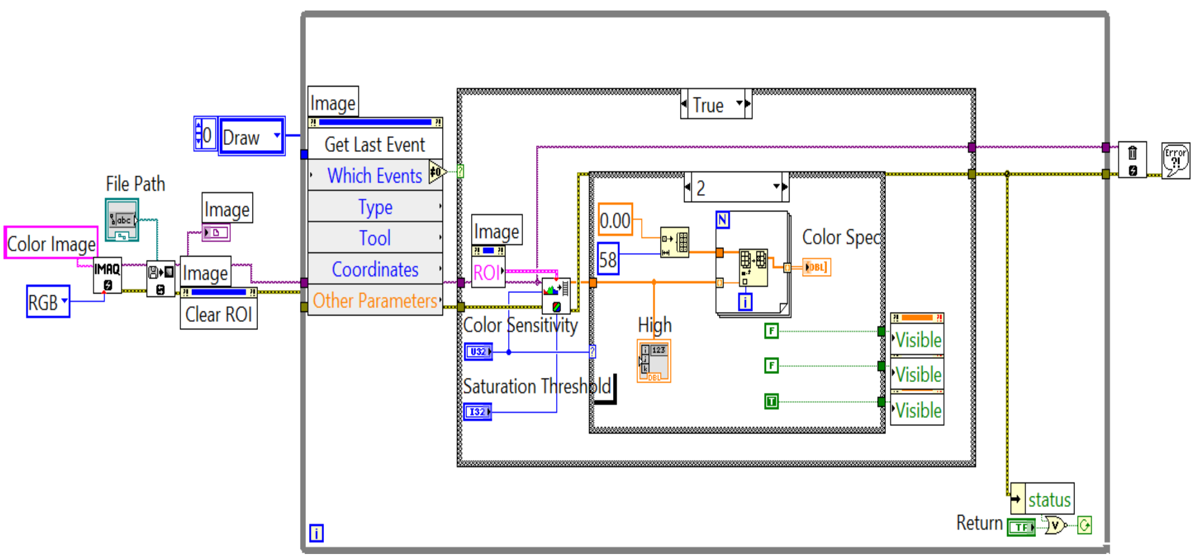

(a)

Preprints (www.preprints.org) | NOT PEER-REVIEWED | Posted: 6 July 2022 doi:10.20944/preprints202207.0094.v1

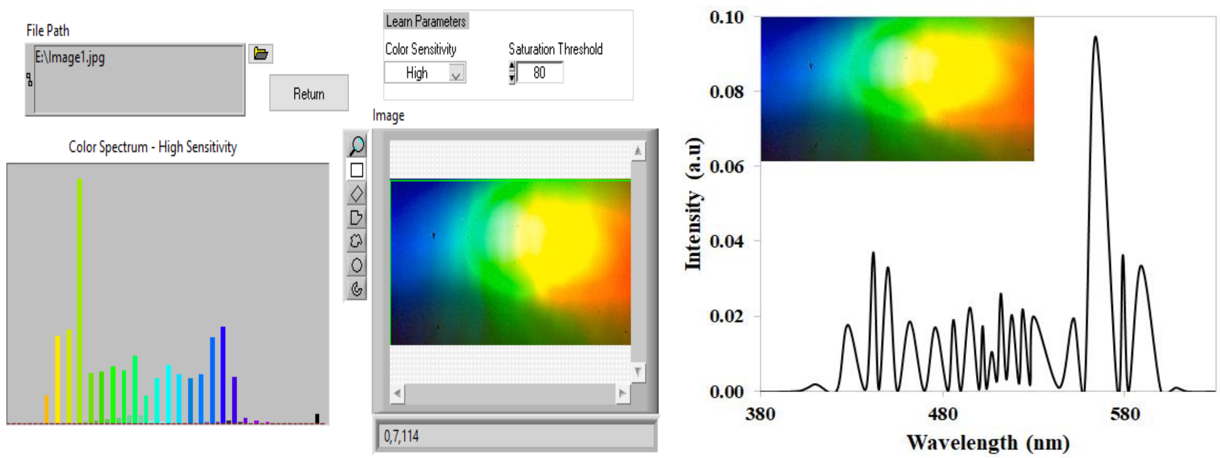

(b) (c)

Fig. 5: (a) Block diagram of the program for the color spectrum of RGB image **(b)** Color spectrum of RGB image [Front Panel] **(c)** Wavelength-Intensity spectrum [FWHM: in the blue region is 6.1 nm, green region is 5 nm, yellow region is 6 nm]

Inside the second case structure, we have used a for loop and arrays to store the intensities corresponding to the different colors. The x-axis of the spectrum contains the number of colors, and the build-in property of the VI fixes the order of color. The y-axis gives the intensity (number of pixels) of the color in the image. Waveform graph VI is used outside the for loop to collect the data stored in the array and plot it in graphical form. IMAQ Dispose and Error Handler VI are placed outside the loop to remove the portion of the image that is not running in the loop [20, 21].

The above Fig. 5(c) shows the spectral profile of each wavelength (blue, green, yellow/reddish) acquires through the image acquisition program in NI LabVIEW. The wavelength-intensity graph is plotted by exporting the data acquired through NI LabVIEW. The spectral fringes are observed due to the interference of wavelength. Simulation results are compared with experimental results showing good agreement.

7. CONCLUSION

An optical spectrometer is designed, simulated and constructed using a diffraction grating and CCD WebCAM as a detector. The designed simulation of an optical imaging spectrometer is carried out in OpticStudio. Different programs are designed using NI LabVIEW tools to capture the image of the spectrum obtained at the detector. The experimental results in the form of images are converted into graphical form by using different VI's in LabVIEW. The result of the spectrometer is analyzed to get an array of pixels and pixel-to-pixel information of the captured image in graphical form. A LabVIEW program is used to get an intensity-wavelength graph of the results captured in the form of an image. Simulation and experimental measurements of the imaging spectrometer are in good agreement. This study highlights the potential of building low-cost efficient imaging spectrometers for laboratories with limited sources.

DATA AVAILABILITY

The data that supports the findings of this study are available within the article [and its supplementary material].

CONFLICT OF INTEREST

On behalf of all authors, the corresponding author states that there is no conflict of interest.

REFERENCES

1. Masson, C. R. "A stable acousto-optical spectrometer for millimeter radio astronomy", Astronomy and Astrophysics, Vol.114, pp.270, (1982).

2. Arzhantsev, S., and Mark Maroncelli. "Design and characterization of a femtosecond fluorescence spectrometer based on optical Kerr gating", Applied Spectroscopy, Vol.59(2), pp.206-220, (2005).

3. Herrera-Martínez, G., et al. "A Design of an Acousto-Optical Spectrometer", Revista Mexicana de Astronomía y Astrofísica, Vol.37, pp.156-159, (2009).

4. Feng, Lei, Lidong Wei, Lei Yang, Xiaoying He, and Jinsong Zhou. "Modeling and Simulation of spectrometer based on prism", In Proceedings of the 2019 8th International Conference on Software and Information Engineering, pp.132-135, (2019).

5. Xu, D., Sui, C., Tong, J., & Yang, H. "Optical Design of Micro Spectrometer", In 2012 Second International Conference on Instrumentation, Measurement, Computer, Communication and Control, pp.339-341, IEEE, (2012).

6. Kim, Seo Hyun, et al. "Design and construction of an Offner spectrometer based on geometrical analysis of ring fields", Review of Scientific Instruments, Vol.85(8), pp.083108, (2014).

7. Micó, Gloria, et al. "Integrated optic sensing spectrometer: Concept and design", Sensors, Vol.19(5), pp.1018, (2019).

8. Naeem, M.; Fatima, N.-u.-a.; Hussain, M.; Imran, T.; Bhatti, A.S. "Design Simulation of Czerny–Turner Configuration-Based Raman Spectrometer Using Physical Optics Propagation Algorithm", Optics, Vol.3, pp.1–7, (2022).

9. Kao, C. F., Lu, S. H., Shen, H. M., & Fan, K. C. "Diffractive laser encoder with a grating in Littrow configuration", Japanese Journal of Applied Physics, Vol.47(3R), pp.1833, (2008).

10. Nagdive, A., Dongre, M., & Makkar, R. "Design and simulation of NIR spectrometer using Zemax", In 2017 International Conference on Innovations in Information, Embedded and Communication Systems (ICIIECS), pp.1-5, (2017).

11. Zemax (An Ansys Company), OpticsAcademy (Optics Studio) [Link]

12. Bergström, Edmund T., et al. "A charge-coupled device array detector for single-wavelength and multiwavelength ultraviolet absorbance in capillary electrophoresis", Analytical chemistry, Vol.71(19), pp.4376-4384, (1999).

13. Muddasir Naeem and Tayyab Imran. "Design and Simulation of Mach-Zehnder Interferometer by Using ZEMAX OpticStudio". Acta Scientific Applied Physics, Vol.2(3) (2022).

14. Kalkman, Cor J. "LabVIEW: A software system for data acquisition, data analysis, and instrument control", Journal of clinical monitoring 11, Vol.1, pp.51-58, (1995).

15. Liao, H. Q., Z. R. Qiu, and G. H. Feng. "The design of LDF data acquisition system based on LabVIEW", Procedia Environmental Sciences, Vol.10, pp.1188-1192, (2011).

16. Wang, Weilin, et al. "Development of software for spectral imaging data acquisition using LabVIEW", Computers and electronics in agriculture, Vol.84, pp.68-75, (2012).

17. Rojas-Laguna, R., et al. "Implementation of a laser beam analyzer using the image acquisition card IMAQ (NI)", 4th Iberoamerican Meeting on Optics and 7th Latin American Meeting on Optics, Lasers, and Their Applications. International Society for Optics and Photonics, Vol.4419, pp.301-304, (2001).

18. Hussain, Mukhtar, and Tayyab Imran. "Design and characterization simulation of Ti: Sapphire-based femtosecond laser system using Lab2 tools in the NI LabVIEW", Microwave and Optical Technology Letters, Vol.60(7), pp.1732-1737, (2018).

19. Imran, T., M. Hussain, and G. Figueira. "Computer-controlled multi-shot frequency-resolved optical gating diagnostic system for femtosecond optical pulse measurement." Microwave and Optical Technology Letters, Vol.59(12), pp.3155-3160, (2017).

20. Klinger, "Thomas. Image processing with LabVIEW and IMAQ Vision", Prentice Hall Professional, (2003).

21. Imran, Tayyab, and Mukhtar Hussain. "An overview of LabVIEW-based f-to-2f spectral interferometer for monitoring, data acquiring and stabilizing the slow variations in carrier-envelope phase of amplified femtosecond laser pulses", Optik, Vol.157, pp.1177-1185, (2018).